CHEMISTRY & CHEMICAL TECHNOLOGY

Vol. 10, No. 4(s), 2016 Chemistry

Boris Minaev

PHOTOCHEMISTRY AND SPECTROSCOPY OF SINGLET OXYGEN IN SOLVENTS. RECENT ADVANCES WHICH SUPPORT THE OLD THEORY

Chemistry and Nano-Material Science Department,
Bogdan Khmelnitsky National University, Cherkasy, 18031, Ukraine

Received: October 22, 2016 / Revised: October 29, 2016 / Accepted: November 10, 2016

Abstract. Molecular oxygen is a paramagnetic gas with the triplet $O_2(X\,^3\Sigma_g^-)$ ground state which exhibits just sluggish chemical reactivity in the absence of radical sources. In contrast, the excited metastable singlet oxygen $O_2(a^1\Delta_g)$ is highly reactive; it can oxygenate organic molecules in a wide range of specific reactions which differ from those of the usual triplet oxygen of the air. This makes the singlet oxygen an attractive reagent for new synthesis and even for medical treatments in photodynamic therapy. As an important intermediate $O_2(a^1\Delta_g)$ has attracted great attention of chemists during half-century studies of its reactivity and spectroscopy, but unusual properties of singlet oxygen makes it difficult to unravel all mysterious features. The semiempirical theory of spin-orbit coupling in dioxygen and in collision complexes of O_2 with diamagnetic molecules proposed in 1982 year has explained and predicted many photochemical and spectral properties of dioxygen produced by the dye sensitization in solvents. Recent experiments with direct laser excitation of O_2 in solvents provide a complete support of the old theory. The present review scrutinizes the whole story of development and experimental verification of this theory.

Keywords: singlet oxygen, spin-orbit coupling, charge-transfer configurations, perturbation theory, electronic-to-vibration energy transfer.

1. Introduction

At the beginning of XX century Oscar Raab in Munich had discovered that the dye-colored cells perished upon lighting. This phenomenon was called "photodynamic action" in order to be distinguished from the photo-sensitization in photography [1, 2]. It was shown soon that the presence of oxygen is necessary for observation of photodynamic action with erythrocyte cells and the active dyes possess intense fluorescence; for all that, the light wavelengths for the photodynamic action excitation coincided with the dye absorption spectrum [1]. The molecular oxygen involvement through the dye photo-sensitization became evident. The primary stage of photodynamic action was proposed to be similar to photo-oxidation observed in biological solvents [1]. The hypotheses of primary photo-dehydrogenation, "molo-xide" and "active oxygen" became popular and were discussed during long time [1-3]. G. Schenck [1] divided all such photoreactions in two types. Type I embraces those reactions which primary stage includes photo-dehydrogenation of the oxidation substrate; type II – reactions of oxygen transfer with the primary stage of complex formation ("moloxide") between O_2 and excited dye. Latter on C. Foote [3] modified this classification: type I includes all reactions where the primary stage is the free-radical formation from excited photo-sensitizer; type II refers to those processes which include interaction of excited photo-sensitizer with oxygen as a primary act. This Foote's classification is commonly accepted now and an interest to the type II reactions is growing [1-6].

Oxidation of alcohols photo-sensitized by ketones is the best example of the type I photoreactions [1, 2]. The primary stages of such processes can be presented by the following scheme [1]. First we have excitation of photo-sensitizer *M* into the excited state *M**:

$$M \xrightarrow{h\nu} M^* \qquad (1)$$

Next we have an electron transfer and free radicals formation including perhydroxyl:

$$\begin{aligned} &M^* + RH \rightarrow {}^{\bullet}M^- + {}^{\bullet}RH^+ \rightarrow {}^{\bullet}MH + R^{\bullet} \\ &{}^{\bullet}M^- + O_2 \rightarrow M + {}^{\bullet}O_2^- \\ &{}^{\bullet}MH + O_2 \rightarrow M + HO_2^{\bullet} \\ &R^{\bullet} + O_2 \rightarrow RO_2^{\bullet} \end{aligned} \qquad (2)$$

where $^{\bullet}M^{-}$ and $^{\bullet}MH$ are free radicals produced under photo-reduction of sensitizer *M*; *RH* is the substrate molecule (alcohol); $R^{\bullet}, RO_2^{\bullet}$ and $^{\bullet}RH^{+}$ are free radicals produced under substrate oxidation. Thus, reactions of type I produce superoxide anion and perhydroxyl radicals ($HO_2^{\bullet}$) which can effectively oxidize bio-substrates [1] and can generate hydrogen peroxide upon dismutation: $HO_2^{\bullet} + HO_2^{\bullet} \rightarrow H_2O_2 + O_2$. The singlet excited oxygen can be produced in this process as well [3]. Reactions of superoxide anion with the hydrogen peroxide provides even more strong oxidizer - hydroxyl radical; this Haber-Weiss cycle can be catalyzed by iron ions [5]:

$$^{\bullet}O_2^{-} + H_2O_2 \xrightarrow{Fe(III)} O_2 + OH^{-} + HO^{\bullet} \qquad (3)$$

The $R^{\bullet}$ radicals produced by the primary substrate dehydrogenation are able themselves to oxidize other organic substrates. By the oxygen addition they can produce $RO_2^{\bullet}$ radicals which are highly reactive and provide dark oxidation of alcohols, ethers, organic acids, hydrocarbons and lipids [1-3]. In such chain reactions the organic peroxides are produced and their decomposition in the Haber-Weiss cycle provides new $HO^{\bullet}$ and $RO^{\bullet}$ radicals which leads to the branched chain processes and to acceleration of organic substrate oxidation. It is known that disproportionation of the peroxide radicals can be accompanied by formation of the intermediate cyclic peroxide of low stability [6] which easily dissociates to carbonyl molecules. Such process can lead to excited carbonyls and oxygen molecule and accompanied by hemiluminescence [6].

Before consideration of the type II photo-processes which include interaction of excited photo-sensitizer with oxygen as a primary step we need to pay attention to such quantum property of electron like “spin”. This is a key word in chemistry since any reaction and any chemical bond can not be understandable without spin account in terms of quantum mechanics [5]. But chemical science was developing during many centuries before the quantum era has begun in 1927. (Though chemistry has pure quantum background, its long development as empirical and phenomenological science was quite successful without spin account, because of beautiful chemical intuition which operates notions “valence”, “affinity”, “oxidation” and other useful concepts being commonly accepted without exact definition). Spin of the ground state of the molecule even nowadays remains as a non-necessary definition especially in organic chemistry. The reason is simple: almost all organic species possess an even number of electrons which are paired on the occupied orbitals according to the Pauli principle [4]. Such molecules have zero spin and the singlet ground state. They do not possess magnetic moment and hence are diamagnetic species [5]. The most important exclusion from such generalization is represented by oxygen [3]. In spite of even number of electrons ($n = 16$) the O_2 molecule possesses two non-paired electrons with parallel spins [7]; thus, it has a total spin quantum number $S = 1$ (triplet state) and a magnetic moment equal to $\sqrt{2}e\mathbf{h}/mc$. Hence O_2 is a paramagnetic species [7].

Paramagnetism of molecular oxygen gas has been discovered by Faraday with magnetic weigh balance in 1848. This result was explained only in 1928 [7]. The O_2 molecule possesses the ground triplet state $X\,^3\Sigma_g^-$ as molecular orbital (MO) theory established [7]. This represents the normal oxygen from the air. The MO theory also predicted the existence of two low-lying singlet excited states $a^1\Delta_g$ and $b^1\Sigma_g^+$ [7] which were observed in sun light absorption of the Earth atmosphere at 1270 and 760 nm, respectively [8]. The second singlet excited state $O_2(b^1\Sigma_g^+)$ with an energy of 1.63 eV occurred to be well known spectral feature of air. It is responsible for the $X\,^3\Sigma_g^- \rightarrow b^1\Sigma_g^+$ absorption transition which determines the most intense red Fraunhofer line at 762 nm [9]. The $X \rightarrow b$ transition is triply forbidden (by spin, inversion and orbital angular momentum symmetry). It is exhibited as magnetic dipole transition being forbidden by spin selection rule. In spite of its low probability the $X \rightarrow b$ transition is well seen in the sun light absorption because of the long path way in the Earth atmosphere. The $X\,^3\Sigma_g^- \rightarrow a^1\Delta_g$ transition is also triply forbidden in electric-dipole approach (by spin, inversion symmetry and by orbital angular momentum change $\Sigma - \Delta$) but in this case the prohibitions are much more severe [10, 11]. It is less intense than the $X \rightarrow b$ transition and has been observed with sensitive spectrometer in the near IR region [8] just after the Mulliken’s prediction. Another important impact of the Mulliken’s paper [7] was connected with the type II photo-processes origin discovery [12].

At this point we need to return to type II photo-reactions. Hydroperoxide formations or oxygen cyclo-addition to alkenes and to aromatic hydrocarbons were observed in photosensitized reactions in the presence of sensitizers (porphyrins, chlorofiles and other dyes) [1-3]. Kinetics of such processes had led to idea of the intermediate “moloxide” formation between O_2 and photo-sensitizer [1]. This idea was considered as an extrapolation of the Bach theory of bio-oxidation with intermediate peroxides [5]. On the basis of the Mulliken’s prediction [7] H. Kautsky has put forward a hypothesis that type II photodynamic actions can be explained by highly reactive $O_2(a^1\Delta_g)$ species generated in energy

transfer process from excited M* photo-sensitizer molecule to the "normal" triplet gaseous oxygen [12]. H. Kautsky has proved his hypothesis by a perfect experiment and detected substrate photo-oxidation when the photo-sensitizer and substrate molecules were adsorbed on opposite grains of silica gel [12]. Thus, it was shown that the mysterious "moloxide" intermediate in photodynamic reactions occurred to be an excited O_2 from the air. By this experiment Kautsky convinced himself in importance of singlet oxygen for photosensitized oxygenation but did not convince other colleagues. His ideas were forgotten for a long time [1], but occurred to be renovated in 1964 when the singlet $a^1\Delta_g$ oxygen was definitely fixed by dimole emission detection [1, 3]. The $O_2(a^1\Delta_g)$ was generated in gaseous microwave discharge and in highly exothermic process in liquid ($NaOCl + H_2O_2$); the products of the subsequent reactions with hydrocarbons (substrates of the type II photo-oxygenation) occurred to be the same as in the photo-processes [3] with similar kinetics [13]. Thus, the idea of Kautsky was completely supported [3, 12-16]. The final prove of the photo-sensitized generation of singlet oxygen in type II photo-reactions was the observation of $O_2(a^1\Delta_g)$ emission at 1270 nm ($a \rightarrow X$) in pigments and dye containing solvents of deuterated water by Krasnovsky, junior [16].

Luminescence of singlet $a^1\Delta_g$ oxygen in solvents is difficult to observe because of fast quenching of the excited O_2^* molecules by solvent vibrations [2, 13-20]. The stationary concentration of singlet O_2^* in solvents is very low as well as intensity of the $a \rightarrow X$ emission; thus, a highly sensitive cooled photomultiplier (FEU-83) [13-18] or Ge-photodiode are necessary for its detection [25-32]. The low radiative rate constant (k_r) for 1270 nm $a \rightarrow X$ emission at low pressure in gases [21] and its essential enhancement in solvents [15, 18] have been explained in a number of old papers [10, 22, 23]. Nowadays the total theoretical backgrounds of this theory are supported by numerous experimental studies [26-32] including recent experiments [33-38] on direct oxygen excitation. Thus, it can be interesting to present a short review of such backgrounds accounting a great importance of singlet oxygen photochemistry in solvents for modern medical diagnostics and therapy [39, 40] as well as for some braches of chemical technology [5, 32].

2. The Old Theory of Singlet Oxygen Spectra in the Low-Pressure Gas Phase

A simple scheme of three low-energy states in the oxygen molecule and all possible electronic transitions between them are presented in Fig. 1. The corresponding emission and absorption bands intensity analysis touches upon the most fundamental principles of physical chemistry: the role of spin and spin-orbit coupling in light interaction with molecules in reactive media, charge-transfer and exchange interactions, solvent theory, *etc*. Thus, such analysis is worse to be scrutinized step by step starting with the rarefied oxygen gas.

The ***a-X*** and ***b-X*** transitions in free O_2 molecule are strongly forbidden in electric-dipole approximation and become allowed as magnetic radiation when spin-orbit coupling (SOC) is taken into account [4, 10]. In free O_2 the corresponding magnetic radiation is determined in Fig. 1 by transitions ***1*** and ***3***, respectively. In this approach both transitions can borrow intensity from magnetic dipole transitions $X\,^3\Sigma_g^- - n\,^3\Pi_g$ induced by the orbital angular momentum $L_\pm$ [11]. Additional contribution to the ***a-X*** band intensity comes from the $a^1\Delta_g - n^1\Pi_g$ magnetic transitions, but the total radiative rate constant is still rather low ($k_r^{a\text{-}X} = 2.6 \times 10^{-4}$ s^{-1}) [41-44], which corresponds to a very small observed extinction coefficient $e_{1270} \approx 10^{-6} M^{-1} cm^{-1}$ [4, 34, 35]. This is actually the transition ***1*** in Fig. 1. The similar contributions to magnetic dipole transition ***3*** (Fig. 1) induced by the orbital angular momentum $L_\pm$ are even lower and practically negligible [11]. Thus, the orbital magnetization can not explain the ***b-X*** transition (***3***) probability in free O_2 molecule, which is actually 340 times higher than that for the ***a-X*** transition ($k_r^{b\text{-}X} = 8.9 \cdot 10^{-2}$ s^{-1}) [4]. Explanation of this puzzle was published first in 1978 [10].

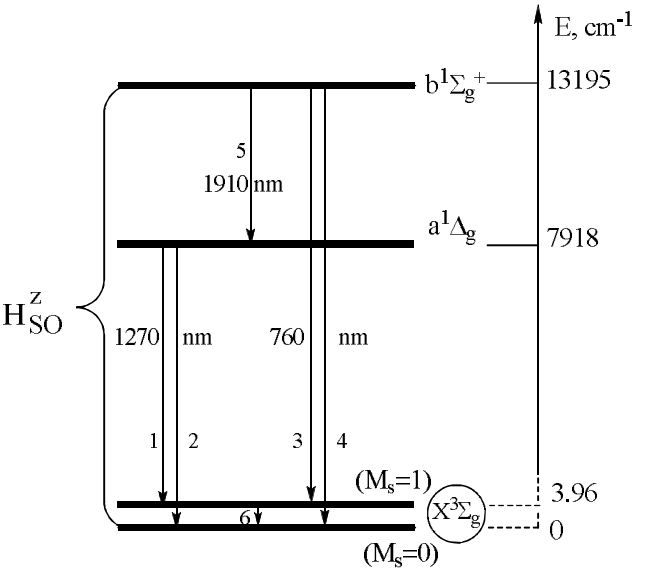

Fig. 1. The energy levels and transitions scheme for oxygen molecule

Index M_s in Fig. 1 is a projection of the spin momentum on molecular axis *z*. It is important to take into account the zero-field splitting (ZFS) in the ground triplet state which is exaggerated in a special scale denoted by dashed lines (D = 3.96 cm^{-1} [9]). This small splitting can be seen in EPR spectra and in high-resolution optical spectroscopy in dilute gases where ro-vibronic lines progressions are well-resolved. For O_2 optics in solvents only wide bands are observed and rotational fine structure is smeared by lines broadening. Thus, no way to distinguish the resolved transitions ***1*** and ***2*** in solvents below the broad band with maximum at about 1270 nm. Nevertheless, in theory one has to consider separately all transitions in O_2 and their response to intermolecular perturbation in solvents. The selection rules for transitions ***1*** and ***2*** and the origin of their intensity in gas and solvents are completely different (the same is true for the ***3*** and ***4*** transitions and for the whole band 760 nm) [10]. In order to see this one has to start with account of SOC in free O_2 molecule by perturbation theory. Let us denote the ground state wave function with M_s=0 as $\left|X\,^3\Sigma_{g,0}^-\right\rangle$ and the perturbed wave functions as $\left|X\,^3\tilde{\Sigma}_{g,0}^-\right\rangle$ (or as a waved symbol $\left|\tilde{\Psi}\right\rangle$ in general). Then one can write the following perturbation theory expressions [4, 10, 11]:

$$\left|b^1\tilde{\Sigma}_g^+\right\rangle = \left|b^1\Sigma_g^+\right\rangle + c_{bX}\left|X\,^3\Sigma_{g,0}^-\right\rangle \qquad (4)$$

$$\left|X\,^3\tilde{\Sigma}_{g,0}^-\right\rangle = \left|X\,^3\Sigma_{g,0}^-\right\rangle - c_{bX} * \left|b^1\Sigma_g^+\right\rangle \qquad (5)$$

where $$c_{bX} = \frac{\left\langle X\,^3\Sigma_{g,0}^-\left|H_{SOC}\right|b^1\Sigma_g^+\right\rangle}{^1E_b - {}^3E_X} = 0.0134 \qquad (6)$$

is a small admixture coefficient, determined by the SOC integral (178 cm^{-1}) [4] divided by the energy gap (13195 cm^{-1}, Fig. 1). Its square is negligible and does not essentially violate the normalization equation $\left\langle\tilde{\Psi}\middle|\tilde{\Psi}\right\rangle = 1$. But the small value in Eq. (6) is extremely important for all photochemistry of singlet oxygen in solvents [4, 23] and for O_2 spectroscopy in atmosphere [10]. Let us note that the SOC integral in Eq. (6) and c_{bX} are real values for the complex MO [4].

Now we need to stress that the magnetic transition ***3*** occurs between the perturbed state $\left|b^1\tilde{\Sigma}_g^+\right\rangle$, Eq. (1), and the sub-state $\left|X\,^3\tilde{\Sigma}_{g,1}^-\right\rangle$ with $M_s = \pm 1$. The transition moments is equal to [10]:

$$\left\langle b^1\tilde{\Sigma}_g^+\middle|b(L_m + 2S_m)\middle|X\,^3\tilde{\Sigma}_{g,1}^-\right\rangle = 2b\left\langle b^1\tilde{\Sigma}_g^+\middle|S_m\middle|X\,^3\Sigma_{g,1}^-\right\rangle =$$
$$= 2b\,c_{b,X}\left\langle X\,^3\Sigma_{g,0}^-\middle|S_m\middle|X\,^3\Sigma_{g,1}^-\right\rangle = \qquad (7)$$
$$= 2b\,c_{b,X} = 0.0268b$$

where $b = e\mathbf{h}/2mc$ is the Bohr magneton; the sub-state $\left|X\,^3\tilde{\Sigma}_{g,1}^-\right\rangle$ wave function is practically pure in contrast to Eq. (5) [4]. Thus, the magnetic transition ***3*** **borrows intensity** from **the microwave transition *6*** (Fig. 1) of the EPR origin [10]. In magnetic dipole operator $b(\hat{L} + 2\hat{S})$ only spin projection (perpendicular to *z* axis) produces non-zero result. The calculated magnetic transition moment (0.0268*b*) exactly corresponds to the observed intensity of the emission band 760 nm in free O_2 molecule ($k_r^{b\text{-}X} = 8.9\cdot10^{-2}$ s^{-1}) [19]. One can note that this intensity is not enhanced much in many solvents [35, 38] which is very interesting in the context of complete approval of the whole theory [23]. The transition ***3*** is a wonderful example of molecular visible band which intensity is determined by spin current contribution [4]. Both singlet oxygen emission bands 760 and 1270 nm in free O_2 are magnetic by nature but they have different origins being determined by spin and orbital angular momentum, respectively. The band 760 nm has no effective sources of intensity enhancement by solvent, but the band 1270 nm can be easily enhanced upon collisions [4].

Transition ***4*** intensity in free O_2 is determined by the permanent quadrupole moments difference for the $b^1\Sigma_g^+$ and $X\,^3\Sigma_{g,Ms=0}^-$ states when they are mixed by SOC perturbation and Eqs. (4)-(6) are taken into account [41, 42]; this difference is very small and equals to 0.38 Debye·Å [32,42]. The calculated transition ***4*** moment $Q_4 = -c_{b,X}(Q_b - Q_X)$ is equal to 0.005 Debye·Å [42]; this corresponds to the radiative rate constant for the $b^1\Sigma_g^+ \rightarrow X\,^3\Sigma_{g,Ms=0}^-$ emission equals to $4.7\cdot10^{-7}$ s^{-1} [42]. Thus, the quadrupole transition ***4*** contribution to intensity of 760 nm band in free O_2 is negligible; it is 10^5 times weaker than transition ***3***. The late determines intensity of this band in absorption and emission spectra for the single O_2 molecule.

The singlet-singlet transition ***5*** (the Noxon band) has also a pure quadrupole nature [20] in low-pressure oxygen gas and is rather weak ($k_r^{b\text{-}a} = 1.7\cdot10^{-3}$ s^{-1}) [4, 21]. The calculated quadrupole transition moment is relatively high and equal $Q_{a,b} = 0.54\,\text{eÅ}^2$ = 2.6 Debye·Å, which corresponds to a small absorption oscillator strength $f_{a,b} = 1.6\cdot10^{-9}$ [41, 44]. Since the transition ***5*** is not spin-forbidden, it becomes very sensitive to the O_2 symmetry reduction by collisions [23]. Calculations of configuration interaction (CI) in MINDO/3 approach [22] provides 10^4 times enhancement of the Noxon band in collision complexes with ethylene since the transition ***5*** becomes electric-dipole allowed in any solvent [23]. Similar enhancement has been obtained in *ab initio* calculations [41]. Intensity of quadrupole transition ***2*** in the rarefied oxygen gas is negligible [20]; in solvents it depends on transition ***5*** enhancement [23]. Thus, both transitions ***2***

and ***4*** in free O_2 molecule (Fig. 1) are of pure quadrupole nature; both are extremely weak and both are determined by SOC mixing, Eqs. (4)-(6). The main difference in a strong response of the 1270 nm band to solvent perturbation and the solvent independence of the 760 nm band intensity can be explained by a difference in the transitions ***2*** and ***4*** behavior in respect to symmetry reduction. Now we can consider this behavior in more details and return to the main purpose of this review – the solvent impact on the singlet oxygen properties.

3. The Old Theory of Singlet Oxygen Emission, Generation and Quenching in Solvents [22]

As it is mentioned in discussion of type II photoreactions, the most popular method of the singlet $O_2(a^1\Delta_g)$ generation in organic solvents is photosensitization (Fig. 2). First we need to excite the dye-sensitizer *M* by elucidation with visible light to the singlet excited state S_1 (dashed arrow, Fig. 2) and then the energy of the excited dye *M**, Eq. (1), will be transferred to the oxygen molecule (k_{ET}) through the intermediate triplet state T_1 involvement [3]. The excited state $O_2(b^1\Sigma_g^+)$ with an energy of 157 kJ/mol (760 nm) can be populated in the first sep of energy transfer from photo-sensitizer; then the $O_2(b^1\Sigma_g^+)$ state relaxes very fast to the $O_2(a^1\Delta_g)$ state (k_i) completing the energy transfer photosensitization process [2, 19]. One can stress that the excited dye *M** can be in the triplet or in singlet excited state. This notion is important for all photochemical reaction. For photo-reaction of type I the triplet dyes are more efficient in terms of total kinetic balance, though the singlet states can also provide some contribution in the yield of oxidation products [1-3]. For type II photo-processes only triplet states are the most reactive in energy transfer. Intersystem crossing in dye (k_{ISC}) should be faster than phosphorescent rate (k_p) [1, 2].

The importance of singlet oxygen photo-reactions in organic and biological solvents requires to understand the solvent impact on the $O_2(a^1\Delta_g)$ lifetime [30-40]. In free O_2 molecule this is just a radiative lifetime ($t_\Delta = 1/k_r^{a-X}$), which is unusually long (about one hour [19]). In solvents the total rate constant for the $O_2(a^1\Delta_g)$ deactivation (k_Δ) embraces all bimolecular processes of singlet oxygen removal [37]:

$$k_\Delta = k_r[S] + k_{nr}[S] + k_q[M] + k_{cr}[M] \qquad (8)$$

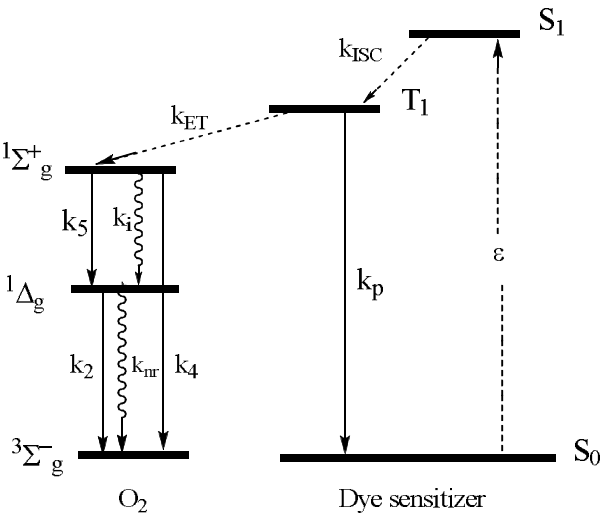

Fig. 2. The processes which are active in singlet oxygen generation by dye containing solvents

where [*S*] is a solvent concentration; [*M*] denotes a concentration of the dissolved molecules (solute) which can be the substrates of oxygenation reaction. The subscript *nr* refers to quenching by solvent, the indexes *cr* and *q* denote the chemical reaction channels and the solute-dependent quenching, respectively.

Both radiative and non-radiative decay of the singlet oxygen $O_2(a^1\Delta_g)$ state can be enhanced by collisions with solvent molecules. But the non-radiative quenching proceeds with much higher rate than the light emission; thus, the non-radiative processes, which include physical and chemical quenching, determine entirely the observed $O_2(a^1\Delta_g)$ lifetime in solvents [24-32]. Since 1964, when Foote had shown [3] that the primary intermediate in the type II photodynamic reactions is the singlet $O_2(a^1\Delta_g)$ species, a huge number of works have been devoted to the rate constants measurements in Eq. (8) [13-19, 24-40]. But the nature of electronic mechanisms besides these processes is still not proper understood [32, 37, 40]. Here we shall concentrate attention on solvent effects, because the k_{nr} rate constant is the most important and mysterious in Eq. (8). In solvents $k_r \approx k_2$ which is much slower than k_{nr}; thus the late constant determines the observed lifetime of the $O_2(a^1\Delta_g)$ state $t_\Delta = 1/k_{nr}[S]$ in the absence of other solutes with chemical quenchers [14, 32].

Nevertheless, we need to understand first the radiative bimolecular rate constant k_r for the $a \rightarrow X$ emission at 1270 nm enhanced by O_2 collision with solvent molecule (*S*), since it is important for k_{nr} origin definition as well. The relatively strong mixing between

$b^1\Sigma_g^+$ and $X^3\Sigma_g^-(M_S=0)$ states induced by SOC, Eqs. (4)-(6), is a key point here. This SOC leads to enhancement of transition ***2*** (Fig. 1): now it can borrow intensity from transition ***5*** which becomes electric-dipole allowed in solvent [22, 23]. The electric dipole transition moment for $a \rightarrow X$ emission ($\boldsymbol{R}_{a,X}$) induced by solvent can be written in a form [23]:

$$\boldsymbol{R}_{a,X} = \left\langle a^1\Delta_g \left| e\mathbf{r} \right| X^3\tilde{\Sigma}_{g,0}^- \right\rangle = -c_{b,X} \left\langle a^1\Delta_g \left| e\mathbf{r} \right| b^1\Sigma_g^+ \right\rangle \quad (9)$$

where the expansion (5) is taken into account; $e\mathbf{r}$ is an electric dipole moment operator.

For free O_2 molecule Eq. (9) is equal to zero and $e\mathbf{r}$ should be substituted by quadrupole moment ($Q = e\mathbf{r}^2$) operator. In fact, the transition ***2*** is of pure quadrupole nature in free O_2 and borrows intensity from the Noxon band. (Transition moments for $a \rightarrow b$ and $b \rightarrow a$ Noxon band are the same by definition). For free oxygen molecule we can substitute in Eq. (9) the $e\mathbf{r}$ operator by operator Q and obtain a similar expression: $Q_{a,X} = -c_{b,X}\, Q_{a,b}$. In this way we have calculated the radiative rate constant of quadrupole transition ***2*** to be practically negligible ($Q_{a,X}$ = –0.072 Debye·Å, $k_2 = 2.3 \cdot 10^{-6}\ s^{-1}$) [20, 44]. This transition is so weak that its intensity was measured just recently with the modern high-sensitive CW-cavity ring-down spectroscopy [21]; it is determined by the radiative rate constant $k_2 = 1.02 \cdot 10^{-6}\ s^{-1}$, which is in a reasonable agreement with our old prediction [20, 44]. The rotational structure analysis [21] completely supports the pure quadrupole nature of this transition ***2*** in free O_2. In spite of the practically negligible intensity of the sub-band ***2***, the unravel of quadrupole nature of this transition in the low-pressure oxygen gas is quite significant for analysis of solvent impact on singlet oxygen emission [20]. In solvents just this transition ***2*** is strongly enhanced by collisions $O_2 + S$ and determines solely the radiative lifetime of the $a^1\Delta_g$ state being close to 5 s in perhalogenated solvents (thousand times enhancement in comparison with free O_2 molecule) [1, 4]. This finding of the enhancement origin is connected in theoretical terms with the mechanism of non-radiative process [20]; the quenching rate of the singlet oxygen was determined successfully in some solvents by account of $Q_{a,X}$ and $R_{a,X}$ transition moments [20, 22].

Let us consider the whole scenario which operates with the O_2 transition rates k_1–k_4 when oxygen is perturbed by random collision with S molecule. The old theory [23] predicts that these photo-physical rate constants of free oxygen are dramatically changed mostly in that part which is connected with the emission at 1.27 μm. Such strong selectivity of the a-X and b-X transitions probability is determined entirely by the different response of quadrupole transitions ***2*** and ***4*** in respect to perturbation by solvent [4]. Both transitions become electric-dipole allowed upon symmetry reduction in collision complex, but magnetic transitions ***1*** and ***3*** are not so sensitive [23, 45]. So far experimentalists have not pay much attention to spin-selectivity of transitions to different spin-sublevels M_s = 0, ±1 [24-36] since they are not resolved in the observed spectra. At the same time the theory of spin-orbit coupling and Eqs. (4)-(6) have predicted from the beginning [23] a strong enhancement of the sub-band ***2***. The transition ***2*** borrows intensity from the Noxon band ***5***, Eq. (9), which becomes electric-dipole allowed in solvent and enhanced few orders of magnitude [23]. This was explained by a small deformation of the molecular oxygen wave functions – $p_{g,x}$ and $p_{g,y}$ molecular orbitals (MOs) [4, 19], which remain quasi-degenerate and localized mainly on O_2 moiety in collision complex [23].

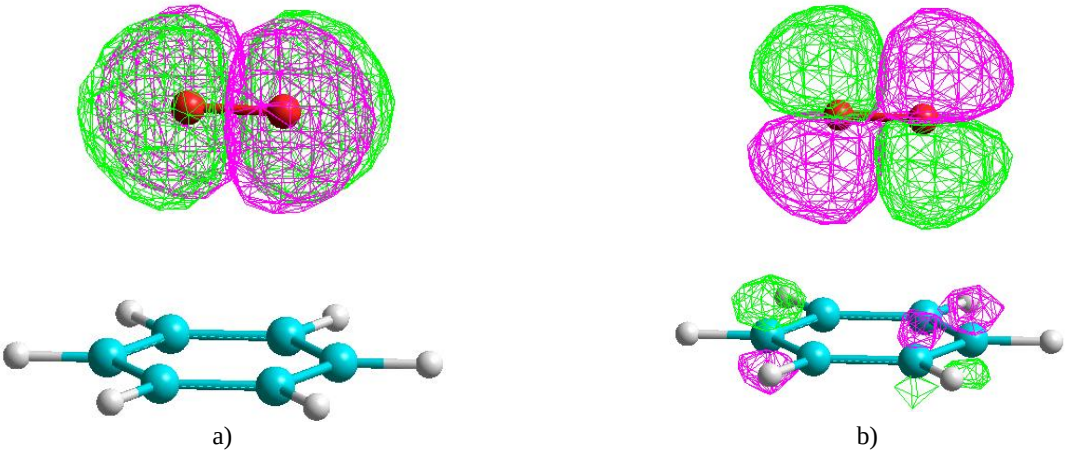

a) b)

Fig. 3. Oxygen open-shell orbitals for collision complex between O_2 and benzene; the $p_{g,y}$ (a) and $p_{g,x}$ (b) molecular orbitals perturbed by collision; the *z*-axis coincides with O–O bond, *xz* plane is close to the symmetry plane, but does not coincide

In Fig. 3a collision complex between benzene and O_2 molecules is shown. Geometry is optimized without symmetry restriction starting from a random geometry of collision at the UB3LYP/6-31G** level [45]. The $p_{g,x}$ MO (Fig. 3b) exhibits some partial charge transfer and delocalization to the solvent molecule, while the $p_{g,y}$ MO (Fig. 3a) remains a pure oxygen orbital. The ***a-b*** band intensity now is determined by electric dipole transition moment (R_5) which is equal to the difference of the permanent dipole moments ($\mu_x - \mu_y$) produced by the $p_{g,x}$ and $p_{g,y}$ molecular orbitals in the collision complex. In spite of a small amount of charge transfer (Fig. 3b), the $p_{g,x}$ MO produces large μ_x value (0.06 Debye) because of long intermolecular distance (3.54 Å), while μ_y = 0 remains unchanged as in free oxygen (thus, $R_5 = .\mu_x$). The calculated oscillator strength for the solvent enhanced Noxon band ($f_{a,b}$ = $9.8 \cdot 10^{-6}$) is about four orders of magnitude higher than that for the free O_2 molecule [23].

3.1. The Role of Solvent Polarity and Polarizability in the 760 and 1270 nm Bands Enhancement

It was shown by many calculations [4] that collision-induced ***a-b*** transition dipole moment R_5 correlates with the solvent refractive index and polarizability [45]. According to Eq. (9) $R_{a,X} = -c_{b,X} R_5$ and the ***a-X*** transition ***2*** borrows intensity from the enhanced Noxon band (***5***), which finally corresponds to a great increase of the calculated oscillator strength up to $f_{a,X}$ = $1.58 \cdot 10^{-9}$ and to the radiative rate constant k_2 = 0.4 $M^{-1} \cdot s^{-1}$. Thus, this is just the transition ***2*** which provides strong enhancement of the singlet oxygen $O_2(a^1\Delta_g)$ emission in solvents while the magnetic transition ***1*** is only slightly changed and remains negligible [45]. All calculations [22, 23] show that the ***a-X*** transition ***2*** probability also should rise in parallel with transition ***5*** and with the polarizability of solvent ***S*** molecule. Hurst *et al*. [25] were the first experimentalists who have noticed that k_r^{a-X} in a number of aromatic solvents grows up with increases of solvent polarizability. This trend is supported by numerous experiments for various solvents [32, 36,40, 46, 47] however, the reason of the phenomenon is not simple [41].

The dipole moment of π_g MO (μ_x) depends on the empty orbitals of the collider and on their response to intermolecular interaction [4, 41]. By this reason it correlates directly with solvent polarizability, since the late is determined by the empty orbitals properties [4, 41]. But this is not true for the transition ***4*** enhancement, which also becomes electric-dipole allowed upon collisions [4, 45]. In free O_2, as mentioned above, the transition ***4*** has a quadrupole nature. Its probability is determined by the permanent quadrupole moments difference between $b^1\Sigma_g^+$ and $X^3\Sigma_{g,Ms=0}^-$ states [when they are mixed by SOC perturbation, Eqs. (4)-(6)] and shown to be negligible [4]. In collision complex with solvent these two states acquire electric dipole moments ($\boldsymbol{\mu_b}$ and $\boldsymbol{\mu_X}$, respectively) and their difference determines the transition ***4*** enhancement by equation: $\boldsymbol{R}_4 = c_{b,X}(\boldsymbol{\mu_X} - \boldsymbol{\mu_b})$. It is obvious that the induced dipoles depend on solvent polarity. For non-polar solvents our calculations [41] predict very small electric dipole transition moment $R_4 \approx 10^{-5}$ Debye. This can not produce any enhancement of the 760 nm band, since the magnetic transition ***3***, Eq. (7), provides much higher intensity. Just the transition ***3*** determines the short radiative lifetime (12 s) of the $b^1\Sigma_g^+$ state in free oxygen molecule [10].

The "dipole — induced-dipole interaction" provides in polar solvents more efficient electrostatic perturbation and transition moment R_4 can be increased up to 10^{-4}–10^{-3} Debye. Its contribution to radiative probability of the $b^1\Sigma_g^+ \rightarrow X^3\Sigma_g^-$ transition at 760 nm is still low but approaches more tightly to the magnetic intensity limit. In experiment with direct oxygen excitation Krasnovsky have found recently a tiny effect of solvent polarity on the extinction coefficient of the 760 nm band [35]; the ***X→b*** absorption band seams to be slightly more intense in polar solvents in agreement with our estimations. All recent experiments [35-38] on direct oxygen excitation are crucial to verify the old theory predictions [23]. Comparison of the absorption intensity of the two bands at 1270 and 760 nm in solvents clearly demonstrates that the former band enhancement (1.27 μm) is much more efficient [35, 38]. It does not depend on polarity of solvent, but depends on solvent polarizability as follows from CI calculations in polar and non-polar solvents [4, 23].

Thus, the role of solvent polarity and polarizability is different for the 760 and 1270 nm bands enhancement: the solvent polarizability does correlate with the electric-dipole transition moment for the 1.27 μm band, but does not – for the red band. In contrast, the late depends slightly only on solvent polarity. One should remind that emission and absorption probability is proportional to the square of transition moment [32]. Thus, Eq. (9) relates the enhancement of the 1.27 and 1.92 μm band intensity in solvents. The squares of electric-dipole transition moments ratio for these bands is proportional to c_{bX}^2 [4, 46] and the measured ratio of radiative rate constants for

these two bands in various solvents is almost constant in agreement with this prediction [32]. The O_2 symmetry violation and electronic structure distortion inside O_2 moiety upon collision do not perturb much the SOC mechanism, Eqs. (4)–(6).

4. The Singlet Oxygen Quenching in Solvents

As follows from many experimental studies, the non-radiative deactivation rate constant k_{nr} in Eq. (8) is the main factor which determines the singlet $a^1\Delta_g$ oxygen lifetime in solvent; the physical quenching is much faster than light emission $k_{nr} >> k_r$ [13-19]. This should testify the different physical mechanism of both bimolecular processes.

Merkel and Kearns [24] proposed in 1972 that the $O_2(a^1\Delta_g)$ excited state electronic energy (89 kJ/mol = = 7918 cm^{-1}) can be quenched and degraded into solvent heating by energy transfer to vibrational degree of freedom in surrounding media. In the inert gases atmosphere the $O_2(a^1\Delta_g)$ is slowly quenched but its decay is much faster in molecular liquids, especially – in organic solvents. The late possess C–H bonds with high frequency of vibrations and provide the quenching rate as large as k_{nr} = 6700 $M^{-1}\cdot s^{-1}$ (in *n*-heptane) [13]. Whereas in argon the $O_2(a^1\Delta_g)$ quenching rate is thousand times slower (k_{nr} = 5 $M^{-1}\cdot s^{-1}$) [32]. In such solvent like chloroform with only one C–H band in *S* molecule the k_{nr} value is intermediate (380 $M^{-1}\cdot s^{-1}$) [13]. From those data Krasnovsky proposed [14] that each C–H stretching mode provides contribution to oxygen quenching accepting some part of oxygen energy. For alcohols he presented the k_{nr} value in the additive form: $k_{nr} = k_{CH} n_H + k_{OH}$, where n_H is a number of hydrogen atoms in solvent molecule [14]. For alkanes the ratio (k_{nr} / n_H) is close to k_{nr} value for chloroform with n_H = 1 (being almost constant). John Hurst *et al*. [25] came to similar additivity ideas independently in the same 1982 year. In a series of fluorbenzene solvents of the type $C_6H_nF_{6-n}$ they have found [26] that the $O_2(a^1\Delta_g)$ lifetime (t_Δ) determined by general equation $1/t_\Delta = k_{nr}[M]$ (and $k_{nr} >> k_r$) decreases linearly with the molar concentration of hydrogen atoms. In general case Eq. (10), which depends on the structure of solvent molecule, was proposed [32]:

$$k_{nr} = \sum_{XY} N_{XY} k_{XY} \qquad (10)$$

where N_{XY} is a number of X-Y bonds in molecule *S*.

To justify Eq. (10) various ideas were considered in terms of vibration mechanics during last three decades [16-18, 25-38]. Unfortunately, the spin-prohibition of non-radiative $a^1\Delta_g \rightarrow X\,^3\Sigma_g^-$ deactivation was not taken into account in most of these works. The classical mechanistic parameters were put into attention such as the Franck-Condon factors (F_m^{ox}) and (F_n^{solv}), the resonance condition (R_{nm}) and collision frequency (*Z*) [29]. The structural dependence of k_{XY} constant was adjusted to these parameters in the form of $k_{XY} = C_\Delta \sum_{mn} F_m^o F_n^{solv} R_{nm}$, where C_Δ – maximum likelihood fitting coefficient [32]. It presumed to take care on implicit account of spin-prohibition. The hard-sphere collisions theory [29] was included into C_Δ parameter in the form of $Z = d^2 N_A (8\pi k_B T / m)^{1/2}$, where all symbols have their ordinary meaning [29]. In Schmidt's approach [29, 32] the C_Δ parameter at room temperature was considered to be a constant value independent of the solvent $C_\Delta = 5.5\times10^5 M^{-1}s^{-1}$. The temperature dependence was included into off-resonance factor R_{nm} [32, 37] and can explain the slow increase of k_{XY} with *T* for few solvents of saturated hydrocarbons measured under photo-sensitized $O_2(a^1\Delta_g)$ generation experiments [14, 32].

The recent direct O_2 excitation measurements (free of dye-sensitizer influence) provide much more accurate detection of t_Δ and k_{nr} values [35] including a temperature range of 278–363 K [36-38]. For a series of solvents (methylated and halogenated benzenes, acetonitrile, alcohols and their deuterated derivatives) the measured temperature dependences $k_{nr}(T)$ are found to be rather peculiar [37]; they can not be explained in terms of the Schmidt's approach [32]. Peter Ogilby *et al*. [37] have proposed recently a new model of singlet oxygen quenching which implies a tunneling through the activation barrier.

They consider the potential energy curves (PECs) for both states, $O_2(a^1\Delta_g)$ and $O_2(X\,^3\Sigma_g^-)$, as functions of O–O bond distance which include the solvent vibration *XY* mode in some implicit way. It is difficult to understand how account of this solvent mode will change so much the PECs of the upper and lower sates and connect them into one PEC along the mysterious reaction coordinate as presented in Fig. 7 of Ref. [37].

The old theory of solvent effects in photo-generation, emission and quenching of $O_2(a^1\Delta_g)$ species, presented thirty years ago [22, 23, 43], can be used to explain the results of recent experiments [35-38].

Unfortunately, the theory of singlet oxygen quenching by amines in gas phase [43] has not been taken into account so far in a great literature on t_Δ measurements and interpretations [29-40]. In the recent papers of P. Ogilby *et al.* [37, 38] a deep understanding of the old theory [11, 23] is achieved and the theory is supported in many details by fine and elaborated laser experiments. Interpretation of external heavy atom (EHA) effect on ***X→b*** transition intensity in terms of different response to solvent of the $M_s = \pm 1$ and $M_s = 0$ transitions (***2, 4*** and ***1, 3***, respectively) explains a very weak enhancement of the ***X→b*** trsnition by all solvents except those which contain halogens and expose the EHA effect [38]. But the explanation of temperature dependences of non-radiative rate constant for ***a→X*** transition [37] is not very consistent since the authors apparently ignore the results of Ref. [43]. First of all, the activation barrier for the $O_2(a^1\Delta_g)$ quenching process, detected by Ogryzlo and Tang [48] in gaseous mixtures with amines, was explained first in Ref. [43]. Then, the old theory [43] considers the role of charge-transfer (CT) states in SOC-induced mixing between $O_2(a^1\Delta_g)$ and $O_2(X^3\Sigma_g^-)$ states. The main point here is the fact that the $O_2(a^1\Delta_g)$ state is doubly degenerate and only one its component is active in the SOC mixing [43]. In Fig. 4 two possible CT states are shown which demonstrate charge transfer from the solvent molecule *M* towards the open shell p_g^2 of oxygen. The *xz* plane in a random collision (Fig. 3) is close to the symmetry plane of the complex and CT states in Fig. 4 differ in respect to this spatial symmetry element.

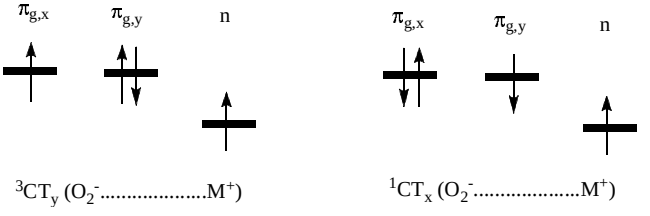

Fig. 4. The charge-transfer states which are active in spin-orbit coupling enhancement

We chose in Fig. 4 the CT states with different spin symmetry in order to stress that they will be admixed to the triplet $O_2(X^3\Sigma_g^-)$ and singlet $O_2(a^1\Delta_g)$ states, respectively. The ^1CT_x state will be always mixed by CI with only one component of the singlet $a^1\Delta_g$ oxygen; the other component will interact by intermolecular CI with the ^1CT_y state (not shown in Fig. 4 but is similar to its triplet counterpart) [43]. Just the ^1CT_x and ^3CT_y states shown in Fig. 4 can strongly interact by SOC:

$$\left\langle {}^1CT_x \left| H_{SOC} \right| {}^3CT_y \right\rangle = \frac{1}{2}\left\langle p_{g,x} \left| B^z \right| p_{g,y} \right\rangle = -\frac{i}{2}V_O \quad (11)$$

where $V_O = 153$ cm^{-1} is the SOC constant for oxygen atom [43]. First of all, in order to produce non-radiative energy transfer from singlet oxygen $O_2(a^1\Delta_g)$ to solvent vibrations both the triplet $O_2(X^3\Sigma_g^-)$ and singlet $O_2(a^1\Delta_g)$ states should be mixed by SOC perturbation. This obstacle was not considered properly in the numerous mechanistic theories of singlet oxygen quenching by solvent [24-30]. Definitely, the solvent must help to overcome the spin prohibition because the triplet $O_2(X^3\Sigma_g^-)$ and singlet $O_2(a^1\Delta_g)$ states in free O_2 do not interact by SOC [4]. Such interaction is assisted by solvent through the charge-transfer CI perturbation: the CT states are admixed to the initial and final states of the quenching process in such a way that SOC mixing between them is allowed by efficient spin-orbit coupling inside O_2 molecule, Eq. (11). We have from Refs. [42, 43] the general mechanism of SOC occurrence in the collision complex: $^1[(^1\Delta_g' ... S_0) + l\,{}^1CT_x(O_2^- ... M^+)] \xrightarrow{SOC} \xrightarrow{SOC} {}^3[(^3\Sigma_g^- ... S_0) + m\,{}^3CT_y(O_2^- ... M^+)]$; this SOC integral is denoted by ω, where $^1\Delta_g'$ is the special component of the singlet oxygen state considered above, which possesses the same spatial symmetry as the ^1CT_x state. The SOC effect on the singlet oxygen quenching depends on lm product, thus it is second-order effect in respect to CT admixtures. Though both values λ and μ are rather small (about 0.2) the effect is still appreciable because of large SOC, Eq. (11). The square of the final SOC integral (ω^2) determines the quenching rate constant k_{nr} and the observed lifetime of $O_2(a^1\Delta_g)$ state in mixed gases and in solvents as well.

The theory of SOC enhancement by CT admixtures [43] was presented for explanation of the singlet oxygen quenching in gas phase by a number of amines with different ionization potentials (IP) [48]. The lifetime of $O_2(a^1\Delta_g)$ decreases with IP of amine and the authors [48] assumed that the charge transfer state $NR_3^+ \ldots O_2^-$ is involved into the quenching process in some unknown way (their arguments were shown to be inconsistent [43]). One has to stress that the overcome of spin prohibition in $O_2(a^1\Delta_g)$ quenching by direct SOC and charge-transfer involvement into the O_2 open shell (Fig. 4) is determined by large SOC inside the O_2 molecule.

The involvement of CT mechanism into the singlet O_2 quenching was assumed before [1, 37, 48, 49] but without proper adjustment. Ogilby *et al.* [37] have cited

the review [3], where the CT mechanism of SOC enhancement [43] was shortly mentioned, without any comments side by side with other references which do not account the degenerate character of $a^1\Delta_g$ state and the SOC mechanism, Eq. (11).

Though the radiative and non-radiative $O_2(a^1\Delta_g) \rightarrow O_2(X^3\Sigma_g^-)$ transitions in free O_2 molecule are heavily spin-prohibited the oxygen molecule itself provides a strong potential to enhance SOC inside its p_g^2 open-shell in response to weak Van-der-Vaals interaction. In order to analyze the $O_2(a^1\Delta_g)$ energy transfer to solvent vibrations we need to consider first the mechanism of cooperative transitions appearance in singlet oxygen emission [55, 56]. A very weak band shifted from 1.27 μm to the long-wave region by the frequency of C–Cl vibration (760 cm^{-1}) in the R_3C-Cl solvents was observed by Chou and Khan [56] and was interpreted as a simultaneous transition in both O_2 and solvent molecules: the $a^1\Delta_g \rightarrow X^3\Sigma_g^-$ emission with simultaneous excitation of the C-Cl vibration.

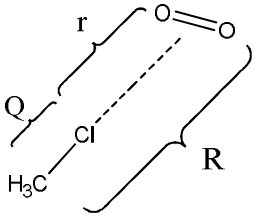

Fig. 5. The model of collision complex between oxygen and chloroform molecules which explains the cooperative transition $a \rightarrow X$ with simultaneously excited C–Cl vibration

Calculations [45, 51-54] show that the CT states are strongly attractive until the equilibrium intermolecular distance $R_e(CT) \approx 2.9$ Å. This distance is not such long in comparison with equilibrium separation $R_e(X)$.= 3.5 Å in the low-lying singlet and triplet states M…O_2. The low-lying states intermolecular potentials have very shallow minima around $R_e(X)$ distance [51], but they can exist during the collision complex lifetime since the intermolecular vibrational quanta are inside the dissociation energy gap [53]. The collision complex model (Fig. 5) demonstrates that the C–Cl vibration (Q mode) at the fixed $R_e(X)$ equilibrium separation leads to modulation of the intermolecular distance (r) between Cl atom and the O_2 molecular center. Even a small reduction of r upon vibration (Fig. 5) can provide a strong rise of the CI coefficients l and m [55]. Thus, the SOC integral between $O_2(a^1\Delta_g)$ and $O_2(X^3\Sigma_g^-)$ states (ω) should be a strong function of the C–Cl vibrational mode [3]. This explains the role of solvent vibration in non-radiative $O_2(a^1\Delta_g) \rightarrow O_2(X^3\Sigma_g^-)$ quenching as well as in the cooperative transition [55]. The rate of quenching is determined by the square of the SOC ω integral:

$$w(r) = w(Q_0) + (\frac{\partial w}{\partial Q})_{Q_0}(Q - Q_0) \qquad (12)$$

where $Q = R\text{-}r$ is the C–Cl vibrational mode and the Q_0 is the equilibrium coordinate of this mode.

The radiative probability for the simultaneous $O_2(^1\Delta_g, v=0) \rightarrow O_2(X^3\Sigma_g^-, v=1)$ transition in oxygen and in solvent shifted from 1.27 μm to the long-wave by the C–Cl vibration frequency is determined according to Eq. (9) by transition moment $-c_{b,X}(\partial\langle a|e\mathbf{r}|b\rangle/\partial Q)_0\langle 0|Q|1\rangle$, where 0 and 1 are vibrational wave functions for C–Cl mode Q. The derivative is large since the $O_2(a^1\Delta_g) \rightarrow O_2(b^1\Sigma_g^+)$ transition moment strongly depends on the intermolecular distance R and on the Q mode (Fig. 5). It was estimated by calculations [55] to be equal $(\partial R_S/\partial Q)_0$ =0.037 Debye/Å. According to this estimation [55] the simultaneous cooperative transition at 1.39 μm shows intensity about 100 times lower than that for the 0-0 band 1.27 μm of the $a^1\Delta_g \rightarrow X^3\Sigma_g^-$ transition in quantitative agreement with experimental measurement [56]. This striking success of the old theory [55] provides a confidence in a similar approach, Eq. (12), being applied to analyzes of non-radiative quenching of the singlet oxygen by solvent vibrations. The similar SOC integral, Eq. (12), between $O_2(a^1\Delta_g)$ and $O_2(X^3\Sigma_g^-)$ states with the initial (v = 0) and the final state ($v = m$) of the C–Cl mode in solvent is determined be the similar equation $\langle (v=0|w(r)|(v=m)\rangle = (\partial w/\partial Q)_{Q_0}\langle 0|Q-Q_0)|m\rangle$. The corresponding $0 \rightarrow m$ transition moment in the solvent molecule can be calculated from the overtone infrared intensity of the C–Cl vibration.

The authors of Ref. [48] have written that the occurrence of activation barrier during the singlet oxygen quenching by amines "is realized at that intermolecular distance in the collision complex at which the energy of the repulsive ground state becomes rather close to the energy of the strongly bound charge-transfer states; this causes their maximum mixing" as a result of CI. Our consideration provides great support to this idea and its generalization to all solvents. The high-frequency C–H, N–H and O–H stretching vibrations in organic solvents are known to be very active in the singlet oxygen quenching [24-32]; these vibrational quanta possess enough energy to accept electronic excitation through lower overtones [32]. In the region of activation barrier at $R < R_e$, where the bound CT states are the most close to the S…$O_2(a^1\Delta_g)$ potential, the X–H vibration experience a strong hindrance (a repulsive part of these vibration potentials are quite steep) and require additional energy (activation barrier). This stipulates a rather strong

dependence of SOC integral w on the hindered normal mode Q displacement. The $w(Q)$ function increases with prolongation of the Q displacement (Fig. 5). The SOC integral $w(Q)$ reaches a maximum at the largest amplitude of X–H vibration. The calculated $w(r)$ are strong functions of intermolecular distance r for various models of tight collisions [4, 43, 55].

From our previous calculations it follows that the oxygen and solvent vibrations both can participate in the electronic energy transfer to solvent vibrations upon the $a^1\Delta_g \rightarrow X^3\Sigma_g^-$ nonradiative quenching [41, 53, 54], which is in agreement with experiments [25-30] and their phenomenological treatments [32]. The $O_2(a^1\Delta_g)$ electronic energy can be shared by both O_2 and solvent vibrations in promoting $O_2(a^1\Delta_g)$ quenching and then transfer vibrational energy to all degrees of freedom in solvent. Both O–O and X–Y modes are active in overcoming the spin-prohibition for the $a^1\Delta_g \rightarrow X^3\Sigma_g^-$ nonradiative transition [53]. They both can promote an effective mixing of initial and final states with charge-transfer configurations (Fig. 4). Thus, these vibrations can induce the SOC integral, Eqs. (11)-(12) and promote the first step of electronic energy transfer into vibrational energy as it was considered in mechanistic scheme of Rainer Schmidt [29, 32]. For example, C–H stretching vibrations of hydrocarbon solvent S being excited in the first step of electronic energy degradation processes can easily transfer their excitation into various C–H and C–C bending modes since all these modes are coupled in the force field of whole molecule. In order to understand the theoretical concept behind Eq. (10) one can not think that the singlet $O_2(a^1\Delta_g)$ species being in collision with S molecule of the solvent is in the force field of all C–H bonds of the S molecule. The number of C–H bonds in Eq. (10) is important since all C–H vibrations are involved in dissipative energy degradation. All C–H stretching modes are mixed through CCH angles deformation and vibrations of C–C skeleton. The larger number of C–H bonds the higher density of vibrational states at resonance and the faster energy dissipation process. The late can involve low-frequency molecular vibrations in THz region, O_2 rotation and solvent phonons. We can consider the oxygen and solvent X–H stretching vibrations as a driving force of the $a \rightarrow X$ quenching process which triggers various dissipative mechanisms.

5. Conclusions

The realm of chemical phenomena in which the singlet $a^1\Delta_g$ oxygen participates is now great and wonderful [39, 40, 57] with most applications in medicine [58-62]. Thus, it is important to know all physicochemical factors determining the $O_2(a^1\Delta_g)$ lifetime in various environments, especially in biological solvents [40, 59]. Extensive experimental studies during last five decades [1-3] provide huge information and its systematization attempts occur often in various reviews [1, 19, 27, 32, 40, 61-64]. But some key electronic mechanisms of $O_2(a^1\Delta_g)$ decay are still poor understood [4, 5]. The old theory of singlet oxygen spectra in gas phase [10, 43] and in solvents [23] has explained a number of SOC-dependent phenomena and predicted new effects which have been recently observed [35-38]. The present review concentrates attention on forgotten parts [43, 55] of the old theory and shows their utility in explanation of recent findings.

The recent experiments on direct time-resolved detection of $O_2(a^1\Delta_g)$ posphorescence in solvents [33-38] unlike the dye-sensitized singlet oxygen emission studies [47, 32] allow more accurate lifetime (t_Δ) measurement [35, 37] and provide additional support to the old theory [23,43]. They provide a new and stronger dependence of the t_Δ value on temperature. It is determined by non-radiative quenching and energy transfer to solvent vibration (mostly to C-H, N-H and O-H modes of organic solvent molecules). Quantitative analysis of vibrational parameters of these bonds presented before [32] did not consider the spin-forbidden character of such process in explicit form. The present review provides analysis of spin-orbit coupling between the initial singlet and final triplet states and explains the driving force of non-radiative $O_2(a^1\Delta_g)$ decay.

This analysis demonstrates the importance of charge-transfer configurations and of degeneracy of the $a^1\Delta_g$ state; it also shows an origin of activation barrier for the singlet O_2 quenching by collisions. The solvent deuterium isotope effect k_{nr}^H / k_{nr}^D and its temperature dependence were explained recently with account of tunneling through the activation barrier [37]. The analysis presented here demonstrates additional arguments in favor of such idea. Connections between cooperative $O_2(a^1\Delta_g)$-solvent phosphorescence and the quenching mechanism are stressed which explain the role of solvent vibrations in the spin prohibition overcoming for the singlet-triplet $a^1\Delta_g \rightarrow X^3\Sigma_g^-$ transition.

In spite of many $O_2(a^1\Delta_g)$ applications in fine organic syntheses [19, 40] the singlet oxygen was considered to be inconvenient for the large scale chemical industry [5, 66]: together with high chemical reactivity of $O_2(a^1\Delta_g)$ molecule, its reactions are not selective enough for industrial applications. Recent developments of TiO_2

and yttrium oxide photo-catalytic systems [62] demonstrate some perspectives in this respect and could be used for effective photo-degradation of organic substances and similar large-scale chemical cleaning technologies.

References

[1] Krasnovsky A., jr.: Biochemistry-Moscow, 2007, **72**, 1065.
[2] Krasnovsky A.: Ann. Rev. Plant Physiol., 1960, **11**, 363.
[3] Foot C.: Science, 1968, **162**, 963.
[4] Minaev B.: Russ. Chem. Rev., 2007, **76**, 988.
[5] Minaev B.: Chem. Chem. Technol., 2010, **4**, 1.
[6] Belyakov V., Vasil´ev R., Minaev B. *et al*. Izvestiya Acad. Nauk SSSR, Ser. Fiz., 1987, **57**, 540.
[7] Mulliken R.: Nature, 1928, **128**, 505.
[8] Herzberg G.: Nature,1934, **133**, 759.
[9] Fraunhofer L.:Denkshrift. Munchner Academie, 1814-1815, 5.
[10] Minaev B.: Sov. Phys. J., 1978, **21**, 1205.
[11] Minaev B.: Int. J. Quant. Chem., 1980, **27**, 367.
[12] Kautsky H.: Trans. Faraday Soc., 1939, **35**, 216.
[13] Krasnovsky A., Jr.: Photochem. Photobiol., 1979, **29**, 29.
[14] Krasnovsky A., jr.: Excited Molecules [in:] Krasnovsky A., jr (Ed.) Kinetics of Transformations (in Rus.), Nauka, Leningrad 1982, 32-50.
[15] Krasnovskiy A., jr.: Chem. Phys. Lett., 1981, **81**, 443.
[16] Krasnovsky A., jr.: Biofizika, 1976, **21**, 748.
[17] Salokhiddinov K., Byteva I. and Dzhagarov B.: Opt. Spectrosc., 1979, **47**, 881.
[18] Salokhiddinov K., Dzhagarov B., Byteva I. and Gurinovich G.: Chem. Phys. Lett., 1980, **76**, 85.
[19] Kearns D.: Chem. Rev., 1971, **71**, 395.
[20] Sveshnikova E. and Minaev B.: Opt. Spectrosc., 1983, **54**, 542.
[21] Gordon I., Kassi S., Campargue A. *et al.*: J. Quantit. Spectrosc. Radiative Transfer, 2010, **111**, 1174.
[22] Minaev B.: Zh. Prikl. Spectroscop., 1985, **42**, 518.
[23] Minaev B.: Opt. Spectry., 1985, **58**, 761.
[24] Merkel P. and Kearns D.: J. Am. Chem. Soc., 1972, **94**, 7244.
[25] Hurst J., McDonald J. and Schuster G.: J. Am. Chem. Soc., 1982, **104**, 2065.
[26] Hurst J. and Schuster G.: J. Am. Chem. Soc., 1983, **105**, 5756.
[27] Ogilby P. and Foote C.: J. Am. Chem. Soc., 1983, **105**, 3423.
[28] Rodgers M.: J. Am. Chem. Soc., 1983, **105**, 6201.
[29] Schmidt R. and Afshari E.: Ber. Bunsen-Ges., 1992, **96**, 788.
[30] Schmidt R. and Brauer H.-D.: J. Am. Chem. Soc., 1987, **109**, 6976.
[31] Krasnovsky A.: J. Photochem. Photobiol. A, 2008, **196**, 210.
[32] Schweitzer C. and Schmidt R.: Chem. Rev., 2003, **103**, 1685.
[33] Sivery A., Anquez F., Pierlot C. *et al.*: Chem. Phys. Lett., 2013, **555**, 252.
[34] Krasnovsky A., jr., Kozlov A. and Roumbal Y.: Photochem. Photobiol. Sci., 2012, **11**, 988.
[35] Krasnovsky A. and Kozlov A.: J. Photochem. Photobiol. A, 2016, **329**, 167.
[36] Bregnhoj M., Blazquez-Castro A., Westberg M. *et al.*: J. Phys. Chem. B, 2015, **119**, 5422.
[37] Bregnhoj M., Westberg M., Jensen F. and Ogilby P.: Phys. Chem. Chem. Phys., 2016, **18**, 22946.
[38] Bregnhoj M., Kragpoth M., Westberg M. *et al.*: J. Phys. Chem. A, 2016, **120**, in press.
[39] Westberg M., Bregnhoj M., Blazquez-Castro A. *et al.*: J. Photochem. Photobiol. A, 2016, **321**, 297.
[40] Ogilby P.: Chem. Soc. Rev., 2010, **39**, 3181.
[41] Minaev B. and Agren H.: J. Chem. Soc. Faraday Trans., 1997, **93**, 2231.
[42] Minaev B., Murugan A. and Agren H.: Int. J. Quant. Chem., 2013, **113**, 1847.
[43] Minaev B.: Theor. Experim. Chem., 1984, **20**, 199.
[44] Minaev B.: J. Mol. Struct. (Theochem), 1989, **52**, 207.
[45] Valiev R. and Minaev B.: J. Mol. Model., 2016, **22**, 214.
[46] Hild M. and Schmidt R.: J. Phys. Chem. A, 1999, **103**, 6091.
[47] Schurlock R. and Ogilby P.: J. Phys. Chem., 1987, **91**, 4599.
[48] Ogryzlo E. and Tang C.: J. Am. Chem. Soc., 1970, **92**, 5034.
[49] Darmanyan A.: J. Phys. Chem. A, 1989, **104**, 9833.
[51] Minaev B., Mikkelsen K. and Agren H.: Chem. Phys., 1997, **220**, 79.
[52] Minaev B., Lunell S. and Kobzev G.: J. Mol. Struct. (Theochem), 1993, **284**, 1.
[53] Minaev B. and Kobzev G.: Spectrochimica Acta A, 2003, **59**, 3387.
[54] Minaev B., Kukueva V. and Agren H.: J. Chem. Soc. Faraday Trans., 1994, **90**, 1479.
[55] Minaev B.: Theor. Experim. Chem., 1985, **21**, 567.
[56] Chou P.-T. and Khan A.: Chem. Phys. Lett., 1984, **103**, 281.
[57] Reshetnyak O., Koval'chuk E., Skurski P. *et al.*: J. Lumines., 2003, **105**, 27.
[58] Dougherty T., Gomer C., Henderson B. *et al.*: J. Natl. Cancer Inst., 1998, **90**, 889.
[59] Jensen R., Arnbjerg J. and Ogilby P.: J. Am. Chem. Soc. 2012, **134**, 9820.
[60] Usselman R., Hill I., Singel D. and Martino C.: PLoS ONE, 2014, **9**, e93065.
[61] Liu X., Ryabenkova Y. and Conte M.: Phys. Chem. Chem. Phys., 2015, **17**, 715.
[62] Kiselev V., Kislyakov I. and Burchinov A.: Opt. Spectrosc., 2016, **120**, 520.
[63] Minaev B.: Spectrochim. Acta A, 2004, **60**, 1027.
[64] Minaev B., Minaeva V. and Evtuhov Yu.: Int. J. Quant. Chem., 2009, **109**, 500.

ФОТОХІМІЯ І СПЕКТРОСКОПІЯ СИНГЛЕТНОГО КИСНЮ В РОЗЧИНАХ. НЕДАВНІ ДОСЯГНЕННЯ, ЯКІ ПІДТВЕРДЖУЮТЬ СТАРУ ТЕОРІЮ

Анотація. *молекулярний кисень є парамагнітним газом з триплетним $O_2(X^3\Sigma_g^-)$ основним станом, що виявляє слабку хімічну реакційну здатність у відсутності джерел радикалів. Збуджений метастабільний синглетний кисень $O_2(a^1\Delta_g)$, на противагу, високореакційний; він може окиснювати органічні молекули за рахунок цілого ряду специфічних реакцій, які відрізняються від реакцій звичайного триплетного кисню повітря. Тому синглетний кисень став привабливим реагентом для нових синтезів і навіть для медичного застосування у фото динамічній терапії. Як важливий інтермедіат, $O_2(a^1\Delta_g)$ привертає значну увагу хіміків протягом півстоліття досліджень його реакційної здатності і спектроскопії, проте незвичні властивості синглетного кисню викликають труднощі у розумінні його таємничих особливостей. Напівемпірична теорія спін-орбітальної взаємодії в кисні і в комплексах зіткнення O_2 з діамагнітними молекулами, запропонована у 1982 році, пояснила та передбачила багато фотохімічних і спектральних властивостей кисню, який одержують сенсибілізацією барвниками в розчинах. Недавні експерименти з прямим лазерним збудженням O_2 в розчинах повністю підтверджують стару теорію. Цей огляд детально розглядає всю історію розвитку і експериментальної перевірки даної теорії.*

Ключові слова: *синглетний кисень, спін-орбітальна взаємодія, конфігурації з перенесенням заряду, теорія збурень, перенесення електронної енергії на коливання.*